

Dark conductivity and photoconductivity of amorphous $\text{Hg}_{0.78}\text{Cd}_{0.22}\text{Te}$ thin films*

Qiu Feng(邱锋)^{1,2}, Xiang Jinzhong(项金钟)¹, Kong Jincheng(孔金丞)², Yu Lianjie(余连杰)², Kong Lingde(孔令德)², Wang Guanghua(王光华)², Li Xiongjun(李雄军)², Yang Lili(杨丽丽)², Li Cong(李棕)^{1,2}, and Ji Rongbin(姬荣斌)^{2,†}

¹School of Physical Science and Technology, Yunnan University, Kunming 650091, China

²Kunming Institute of Physics, Kunming 650223, China

Abstract: This paper reports the dark conductivity and photoconductivity of amorphous $\text{Hg}_{0.78}\text{Cd}_{0.22}\text{Te}$ thin films deposited on an Al_2O_3 substrate by RF magnetron sputtering. It is determined that dark conduction activation energy is 0.417 eV for the as-grown sample. Thermal quenching is absent for the as-grown sample during the testing temperature zone, but the reverse is true for the polycrystalline sample. Photosensitivity shows the maximum at 240 K for amorphous thin films, while it is higher for the as-grown sample than for polycrystalline thin films in the range from 170 to 300 K. The recombination mechanism is the monomolecular recombination process at room temperature, which is different from the low temperature range. The $\mu\tau$ -product is low in the range of 10^{-11} – 10^{-9} cm^2/V , which indicates that some defect states exist in the amorphous thin films.

Key words: amorphous MCT; dark conductivity; photoconductivity

DOI: 10.1088/1674-4926/32/3/033004

EEACC: 2520

1. Introduction

In recent decades, mercury cadmium telluride (MCT or $\text{Hg}_{1-x}\text{Cd}_x\text{Te}$) has been one of the most vital infrared optoelectronic materials as a result of its outstanding features, such as its long spectral sensitivity wavelength ranges, low dielectric constant and low thermal coefficient^[1–3]. Therefore, there are many reports of relevant research on monocrystalline and polycrystalline MCT thin films in related directions^[4–6]. Considering the product cost for monocrystalline MCT and high absorption coefficient for amorphous MCT, however, there should have been research on a-MCT. Our team has already investigated photoelectric performances of a-MCT^[7,8] on the basis of previous research on HgCdTe material at Kunming Institute of Physics^[9]. In previous investigations, it was shown that HgCdTe materials have a wide range of applications for detectors, thermal image systems to meet the requirements of civil and military operations, and especially showing advantages over focal plane array detector devices. The study of our team on a-MCT mainly concentrates on the amorphous material growth window, annealing modification, transport mechanism, and optical properties that include absorption, transmittance and, reflectance. There are many novel discoveries from our further research on a-MCT's physical performance.

Two types of photoconduction are defined in solids. One is primary photoconduction, which is a time of flight (TOF) technique. In this paper, we adopt the second type of photoconduction in which the whole sample is illuminated and the photocurrent is measured between two electrodes with ohmic contacts. This secondary photoconduction is also known as steady-state photoconductivity (SSPC). Through SSPC measurement it is found that the dark conductivity and photoconductivity of materials vary with temperature and photon flux, photosensitivity

discrepancy among different temperatures, recombination dynamics, and mobility-lifetime of the product. From the data, we further discuss the physical properties of amorphous materials and obtain some mechanisms to analyze the performance of optoelectronic materials, finally improving material parameters through a correlated technique for photoconductive devices.

2. Experimental method

Thin films of amorphous $\text{Hg}_{0.78}\text{Cd}_{0.22}\text{Te}$ were grown by RF magnetron sputtering with low sputtering power on Al_2O_3 substrates. The substrate temperature was kept at 283 K during the growth process. A polycrystalline sample was obtained from annealing at 393 K over crystallization temperature for 1 h in an evacuated quartz ampoule in a vacuum better than 8.0×10^{-4} Torr. Coplanar geometry with Cr (the thickness of Cr is 19 nm) and an Au double layer, which improves the contact characteristic between the Au and the substrate, were fabricated (gap spacing 48 μm , gap width 250 μm) by photolithography and ion beam etching techniques. The ohmic characteristic of the contacts was verified by the straight line passing through the origin of the current–voltage plot. Samples were encapsulated inside a metallic dewar vessel with a transparent ZnS window, in which the vacuum was better than 8.0×10^{-4} Torr. The measurement temperature was varied from liquid nitrogen temperature to room-temperature by means of heating up liquid nitrogen slowly inside a dewar vessel via a temperature controller. The current–voltage (I – V) characteristics, which were analyzed by computer through a self-compiled program, were obtained by using a Keithley 2400s Source Meter. The applied voltage was kept at 10 V, which indicated the electric field intensity 1.72×10^3 V/cm. The conductivity was calculated from the formula $\sigma = (I/V)(L/wd)$ (L , w and d

* Project supported by the National Natural Science Foundation of China (No.60576069).

† Corresponding author. Email: fengqiu2010@gmail.com

Received 3 September 2010, revised manuscript received 20 October 2010

© 2011 Chinese Institute of Electronics

are the gap spacing, gap width and thin film thickness, respectively). The photoconductivity of the thin films was studied in the steady state adopting the He-Ne continuous laser ($\lambda = 632.8$ nm, luminous power = 0.58 mW). Light attenuation was analyzed by utilizing IR filters.

The chemical composition was checked by energy dispersion X-ray analysis (EDAX) using a scanning electron microscope (Phillips). The structure of the thin films was measured by X-ray diffraction (D/Max2200, $\text{CuK}\alpha = 0.15406$ nm, 30 mA, 40 kV). Through XRD analysis, the as-grown sample, which showed two distinctly extended wave packets in the diffraction pattern, was an amorphous structure, labeled No.1. The films through thermal treatment, nevertheless, which reveals several sharp diffraction peaks and show the preferred orientation (111), indicate a polycrystalline sample structure, labeled No.2. The optical absorption and reflectivity spectrum were measured by spectroscopic ellipsometry (SE) (HR460, JOBIN YVON) in the energy range from 0.7 to 4.7 eV. The absorption coefficient, α , and reflectivity, R , were $2.9 \times 10^5 \text{ cm}^{-1}$ and 0.369, respectively. The thicknesses of the samples were determined to be equal to $1.6 \mu\text{m}$ by an advanced stylus profiling system (XP-2). The conduction of carriers in amorphous thin films was electron obtained from the negative Seebeck coefficient.

3. Results and discussion

3.1. Dark conductivity and photoconductivity

Dark conductivity, σ_d , was the direct current (DC) conductivity of thin films under no light lumination condition. Photoconductivity, σ_{ph} , was the additional photoconductivity of the excess number of photogenerated charge carriers under steady-state illumination, which was gained by subtracting dark conduction from the conductivity of lumination, σ_p , that's $\sigma_{ph} = \sigma_p - \sigma_d$.

The dark conductivity and photoconductivity of as-grown and polycrystalline sample of $\text{Hg}_{0.78}\text{Cd}_{0.22}\text{Te}$ were measured as a function of temperature and shown in Fig. 1. It was observed that the dark conduction of the two samples increased with increasing temperature. At the same time it was found to be activated over the different temperature range and follow the Arrhenius equation:

$$\sigma = \sigma_0 \exp\left(-\frac{\Delta E}{K_B T}\right), \quad (1)$$

where σ_0 is the pre-exponential factor, and K_B is Boltzmann's constant. ΔE is the activation energy for dark conduction and calculated from the slope of $\ln \sigma$ versus $1/T$. The results of these calculations are given in Table 1. It is clear that dark conduction activation energy ΔE is higher than photoconductivity activation energy ΔE_{ph} in the temperature range 300–250 K for as-grown thin films labeled No. 1.

Note: σ_{01} and σ_{02} are the pre-exponential factors for dark conductivity and photoconductivity, respectively.

From Fig. 1, we can get that dark conductivity and photoconductivity increase nearly by two orders of magnitude with increasing temperature. Conductivity of polycrystalline sample is higher than that of amorphous one by four orders of magnitude whether dark conductivity or photoconductivity. This

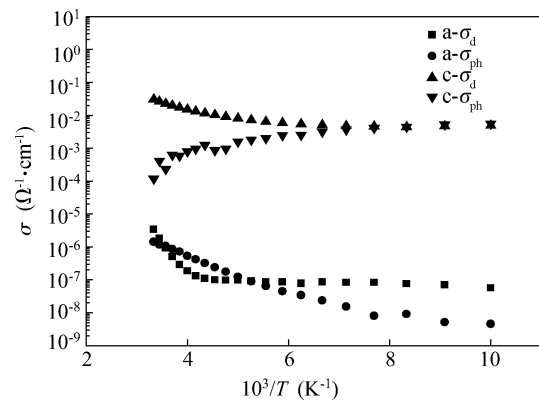


Fig. 1. Temperature dependence of dark conductivity and photoconductivity for amorphous and polycrystalline thin films of a- $\text{Hg}_{0.78}\text{Cd}_{0.22}\text{Te}$.

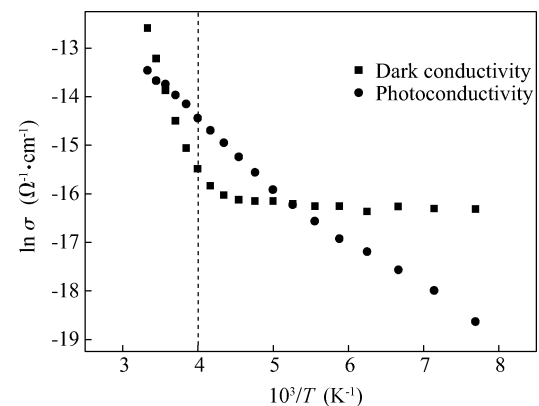


Fig. 2. Conductivity against the inverse temperature for amorphous MCT thin films.

indicates that amorphous material has many defects for its absence of long-range order contrasting with the polycrystalline sample. From Fig. 2, it is obvious that two different transport mechanisms dominate two different temperature zones. The critical temperature is approximately 250 K.

There is another important research for photoconductivity, that's thermal quenching (TQ)^[10], which indicates that photoconductivity decreases with increasing temperature. Thermal quenching of photoconductivity occurs when the minority carriers are excited thermally with rising temperature and transfer to the recombination centers^[11]. From Fig. 1, the photoconductivity of the amorphous sample increases with increasing temperature unvaryingly during the testing temperature range. That is absence of thermal quenching. This is in consonance with a- $\text{Se}_{85}\text{Te}_{15-x}\text{Pb}_x$ thin films^[12], a- $\text{Ge}_x\text{Se}_{100-x}$ thin films^[13]. However, the polycrystalline sample behaves the effect of thermal quenching but absence of the maximum. The appearance of the TQ effect is in accordance with Sanjay *et al.* $\mu\text{c-Si:H}$ ^[14], Tran *et al.* both undoped and doped a-Si:H^[15], Reis *et al.* a-Ge:H films^[16].

3.2. Photosensitivity

An important and useful parameter in photoconductivity measurement is the photosensitivity in a certain temperature

Table 1. Electronic parameters in the amorphous and polycrystalline thin films of MCT.

sample	Temperature range (K)	σ_{01} ($\Omega^{-1} \cdot \text{cm}^{-1}$)	ΔE (eV)	σ_{02} ($\Omega^{-1} \cdot \text{cm}^{-1}$)	ΔE_{ph} (eV)
No.1.	300–250	33.089	0.417	3.23×10^{-3}	0.167
	250–77	1.51×10^{-7}	0.0078	3.97×10^{-6}	0.079

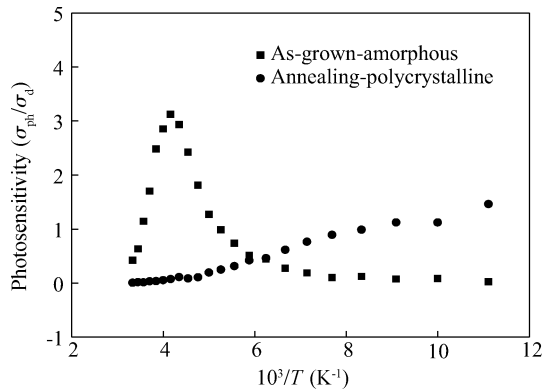


Fig. 3. Temperature dependence of photosensitivity for amorphous and polycrystalline thin films.

range under particular illumination. This is defined by dark conduction divided by photoconductivity, that is $\sigma_{\text{ph}}/\sigma_{\text{d}}$ ^[17]. The value of photosensitivity for a photoelectric material determines the application of the photoconductive devices.

From Fig. 3, we can see that the amorphous thin film shows maximal photosensitivity at 240 K using a He–Ne laser. In the lower temperature range, however, there is only a small amount of photosensitivity and it is near constant for the amorphous sample. Whereas the photosensitivity of the polycrystalline sample decreases with increasing temperature. At high temperature at about 170–300 K, the photosensitivity of the amorphous thin films is higher than that of the polycrystalline sample, and the reverse at low temperature. Dixit reported that this photosensitivity decreased after crystallization on the a-Se₈₀Te₂₀^[18], which is in accord with each other in the high temperature range.

The maximum photosensitivity indicates that the density of the defect states in a-Hg_{0.78}Cd_{0.22}Te thin films is minimal at 240 K^[18, 19].

3.3. Recombination mechanism

The photoconductivity, σ_{ph} , is written as

$$\sigma_{\text{ph}} = eG\tau\mu, \quad (2)$$

where G is the generation rate of the photocarriers in the unit of $\text{cm}^{-3} \cdot \text{s}^{-1}$, τ is the recombination time measured in seconds (s), and μ is the photocarrier mobility [$\text{cm}^2/(\text{V} \cdot \text{s})$] when transport occurs in the extended states. However, μ represents the hopping mobility when transport occurs in the tail states, which is much smaller than the free-carrier mobility. For a thin film of thickness d , neglecting multiple reflections, the generation rate of photocarriers, G , can be written as^[20, 21]

$$G = \eta I_0(1 - R)[1 - \exp(-\alpha d)]/d, \quad (3)$$

where η is the quantum efficiency of the generation of photocarriers, I_0 is the number of incident photons per unit area

Table 2. Exponent and characteristic temperature varying with temperature.

Temperature (K)	Exponent γ	T_c (K)
80	-0.55	97.8
90	-0.6	135
100	-0.08	8.7
110	-0.29	45
120	0.09	11.9
140	-0.41	97.3
300 (RT)	0.986	$\gg 300$

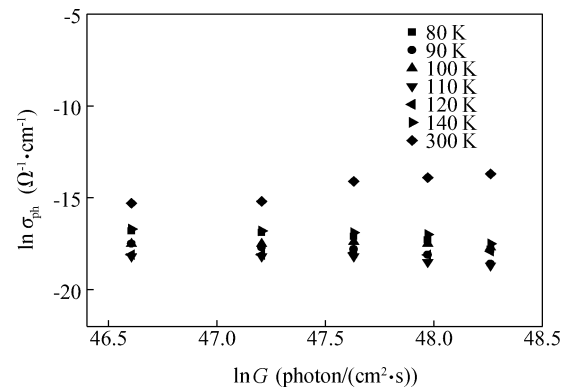


Fig. 4. Generation G dependence of σ_{ph} at different temperatures for the as-grown sample.

($\text{photon}/\text{cm}^2 \cdot \text{s}$), that's photon flux, R is reflectivity, and α is the absorption coefficient.

Generally, it should be noted that G and τ are not independent variables but are dependent on each other for easy consideration. The dependence of τ on G already has gained by Wronski and Daniel as^[22]

$$\tau \propto G^{-(1-\gamma)}. \quad (4)$$

Thereby, from the above discussion we can get

$$\sigma_{\text{ph}} = e\mu G\tau \propto e\mu G G^{-(1-\gamma)} \propto G^\gamma, \quad (5)$$

where γ is the photoconductivity exponent, which determines the recombination mechanism. The value of $\gamma = 0.5$ indicates a bimolecular recombination process, whereas $\gamma = 1$ indicates monomolecular recombination^[23]. However, in many amorphous semiconductors, intermediate values of the exponent γ are found. The occurrence of such values have been extensively discussed and explained by Rose^[24]. The exponent γ lies between 0.5 and 1, which indicates that there exists a continuous distribution of localized states in the mobility gap of amorphous materials.

From Fig. 4 and Table 2, we get the value of γ . However, the anomalous value, which is negative in the low temperature zone, is observed. The negative sign appears due to photoconductivity decreasing with increasing photon flux. This phenomenon shows amorphous thin films generate defect states

transferring to recombination centers during the mobility gap under illumination enhancement. The value γ equals 0.55, which indicates closing to bimolecular recombination for photocarriers in amorphous $\text{Hg}_{0.78}\text{Cd}_{0.22}\text{Te}$ thin films at low temperature, 80 K. The value of γ which is 0.55 and 0.6 at 80 K and 90 K, respectively, indicates that a continuous distribution of localization states exists in the mobility gap. However, the as-grown sample shows a monomolecular recombination process at room temperature. In the interim temperature between 100–140 K, the exponent is found to be sublinear with γ as low as 0.09 at 120 K, which is consistent with Sanjay's experiment on undoping $\mu\text{c-Si:H}$ γ value as low as 0.13^[25], but Sanjay explained that the sublinear behavior of γ (< 0.5) was attributed to the shift of the Fermi level through a localized state distribution.

Amorphous MCT is a very special optoelectronic material for mercury vacancy. This may contribute to an increased recombination rate, resulting in a low γ value of amorphous thin films.

According to Rose, $\gamma = T_c / (T + T_c)$, where T_c is the characteristic temperature. Product, $K_B T_c$, is the characteristic energy of the conduction band tail (CBT). From the T_c , we can determine that the width of CBT is higher at room temperature than that at low temperature.

3.4. $\mu\tau$ -product

In general, photoconductivity depends on both the mobility of carriers μ and the recombination time τ , and hence the $\mu\tau$ -product becomes a very important factor because it is independent of photon flux, film thickness, absorption coefficient and so on. It also determines the performance of photoconductive devices.

In the SSPC measurement, the condition for the steady-state is given by

$$\frac{d(\Delta n)}{dt} = G - \frac{\Delta n}{\tau} = \eta I_0 (1 - R) \frac{1 - e^{-\alpha d}}{d} - \frac{\Delta n}{\tau}, \quad (6)$$

where Δn is the density of photocarriers in cm^{-3} . In the amorphous HgCdTe thin films, it is adopted electron transport. Given the initial conditions, $t = 0$, $\Delta n = 0$ and solving the above equation, the following expression is obtained when the illustration time t is greater than the recombination time τ far and away,

$$\sigma_{\text{ph}} = q\Delta n\mu_n = q\eta I_0 (1 - R) \frac{1 - e^{-\alpha d}}{d} \mu_n \tau_n, \quad (7)$$

where μ_n , τ_n is the photocarrier mobility of the electrons, and the recombination lifetime of the electrons, respectively. From this expression we gain the $\mu\tau$ -product by equating η to unity and plot as follows.

From Fig. 5, it is indicated that the as-grown sample shows the $\mu\tau$ -product range 10^{-11} – 10^{-9} cm^2/V . This is lower than a-Si:H that give 10^{-7} – 10^{-4} cm^2/V in $\mu\tau$ -product from SSPC measurement while gets 10^{-9} – 10^{-7} cm^2/V from TOF test^[20]. The $\mu\tau$ -product that is rather low in amorphous HgCdTe thin films by comparison with a-Si:H thin films shows lots of defects existing in the material by adopting the magnetron sputtering technique.

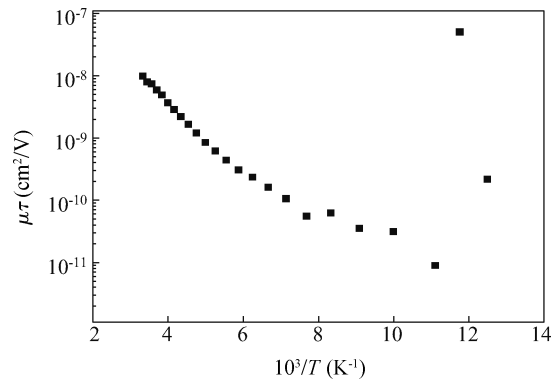


Fig. 5. Mobility-lifetime product versus reciprocal temperature for the as-grown sample.

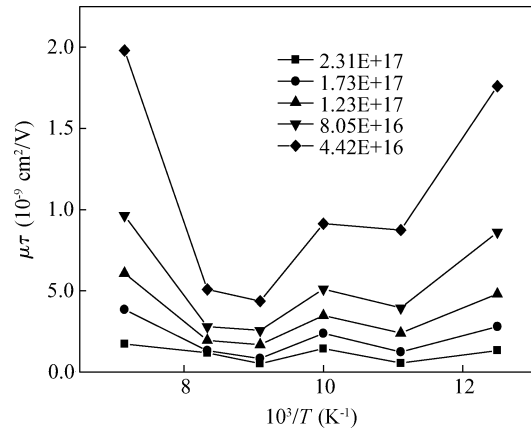


Fig. 6. Temperature dependence of the $\mu\tau$ -product for different photon fluxes for the as-grown sample.

Figure 6 shows that with increasing the photon flux the $\mu\tau$ -product decreases in the low temperature range. This conclusion does not agree with the conventional routine. In general, the $\mu\tau$ -product increases with increasing the photon flux^[14, 23]. This anomalous process indicates that the recombination centers increase with increasing the photon flux, resulting in $\mu\tau$ -product decrease in the low temperature range.

4. Conclusions

From the steady-state photoconductivity measurement we obtain a photocurrent varying with temperature and photon flux. Through corrected calculation we gain dark conductivity and photoconductivity data, and preliminary analysis is acquired. The activation energy is equal to 0.417 eV in the amorphous $\text{Hg}_{0.78}\text{Cd}_{0.22}\text{Te}$ thin films. Amorphous thin films are absent from the thermal quenching effect. The as-grown sample shows maximum photosensitivity at 240 K, which indicates the distribution of defect states with temperature variation. The photosensitivity is higher than that of polycrystalline thin films in the high temperature range. From the exponent γ values, we know that the as-grown sample shows bimolecular recombination at 80 K but monomolecular recombination at room temperature. Anomalous behavior of the exponent γ , which is as low as 0.09, is discovered. Intermediate values of γ between

0.5 and 1 indicate that there exists a continuous distribution of localization states in the mobility gap. The characteristic temperature T_c shows that the width of CBT is higher at room temperature than at low temperatures. The $\mu\tau$ -product, which was calculated from the steady-state photosensitivity, was obtained in the 10^{-11} – 10^{-9} cm²/V range, which indicates that some defect states exist in the amorphous thin films by the magnetron sputtering technique.

References

- [1] Liu M, Man B, Lin X C, et al. Effects of pressure on pulsed laser deposition of HgCdTe films. *Mater Chem Phys*, 2008, 108: 274
- [2] Rogalski A. Infrared detectors: status and trends. *Progress in Quantum Electronics*, 2003, 27: 59
- [3] Longo J T, Cheung D T, Andrews A M, et al. Infrared focal planes in intrinsic semiconductors. *IEEE Trans Electron Devices*, 1978, 25: 213
- [4] Shayegan M, Goldman V J, Drew H D. Magnetic-field-induced localization in narrow-gap semiconductors Hg_{1-x}Cd_xTe and InSb. *Phys Rev B*, 1988, 38: 5585
- [5] Jung J W, Lee H C, Wang J S. A study on the double insulating layer for HgCdTe MIS structure. *Thin Solid Films*, 1996, 290: 18
- [6] Wisz G, Virt I, Kuzma M. Electrical properties of HgCdTe films obtained by laser deposition. *Thin Solid Films*, 1998, 336: 188
- [7] Kong J, Wang S, Kong L, et al. Studies of RF magnetron sputtered amorphous HgCdTe films. *Proc SPIE*, 2009, 7383: 73833Y
- [8] Yu L, Shi Y, He W, et al. Relationship between dark conductivity and temperature for amorphous HgCdTe films. *Proc SPIE*, 2009, 7383: 73833N
- [9] Su J, Zeng G. HgCdTe detector technology at Kunming Institute of Physics. *Proc SPIE*, 1996, 2894: 90
- [10] Pearsans P, Fritzsche H. Dual light beam modulation of photocarrier lifetime in intrinsic a-Si:H. *Journal de Physique*, 1981, C42: 597
- [11] Iiker A Y, Tolunay H. Steady-state and transient photoconductivity in hydrogenated amorphous silicon nitride films. *Solar Energy Materials Solar Cells*, 2003, 80: 209
- [12] Kushwaha N, Shukla R K, Kumar S, et al. Anomalous behaviour in dark conductivity and photoconductivity in a-Se₈₅Te_{15-x}Pb_x thin films at low temperatures. *Mater Lett*, 2006, 60: 3260
- [13] Qamhieh N, Adriaenssens G J. Steady-state photoconductivity in amorphous germanium selenide films. *J Non-Cryst Solids*, 2001, 292: 80
- [14] Ram S K, Kumar S, Cabarrocas P R. Numerical modeling of steady state photoconductivity process in highly crystallized undoped μ c-Si:H films. *Thin Solid Films*, 2007, 515: 7576
- [15] Tran M Q. On thermal quenching of the photoconductivity in hydrogenated amorphous silicon. *Phil Mag B*, 1995, 72: 35
- [16] Reis F T, Comedi D, Chambouleyron I. Temperature dependence of the photoconductivity of gallium-doped hydrogenated amorphous germanium films. *J Non-Cryst Solids*, 2000, 266: 730
- [17] Bube R H. Photoelectronic properties of semiconductors. Cambridge: Cambridge University Press, 1992
- [18] Dixit M, Kumar A. Effect of photocrystallization on the photoconductivity of a-Se₆₅Te₂₀Sb₁₅. *Physica B*, 1998, 252: 286
- [19] Dahshan A, Amerb H H, Moharam A H, et al. Photoconductivity of amorphous As-Se-Sb thin films. *Thin Solid Films*, 2006, 513: 369
- [20] Kakinuma H. Fermi-level-dependent mobility-lifetime product in a-Si:H. *Phys Rev B*, 1989, 39: 10473
- [21] Singh J, Shimakawa K. *Advances in amorphous semiconductors*. London, New York: Taylor & Francis Group, 2003: 250
- [22] Wronski C R, Daniel R E. Photoconductivity, trapping, and recombination in discharge-produced, hydrogenated amorphous silicon. *Phys Rev B*, 1981, 23: 794
- [23] Kamboj M S, Kaur G, Thangaraj R, et al. Structural and transport properties of amorphous Se-Sb-Ag chalcogenide alloys and thin films. *Thin Solid Films*, 2002, 516: 179
- [24] Rose A. *Concepts in the photoconductivity and allied problems*. New York: Interscience, 1963
- [25] Ram S K, Kumara S, Cabarrocas P R. Study of anomalous behavior of steady state photoconductivity in highly crystallized undoped microcrystalline Si films. *J Non-Cryst Solids*, 2006, 352: 1172